ANALYSIS

56(291), March, 2020

ISSN 2278–5469 EISSN 2278–5450

DISCOVERY

Velocity distribution of electrons along the symmetry axis of Quadrupole Penning trap

Dyavappa BM

Department of Physics, Government College for Women, Kolar, India; E-mail: dyavappabm@gmail.com

Article History

Received: 05 December 2019

Reviewed: 09/December/2019 *to* 21/January/2020

Accepted: 24 January 2020

Prepared: 27 January 2020

Published: March 2020

Citation

Dyavappa BM. Velocity distribution of electrons along the symmetry axis of Quadrupole Penning trap. *Discovery*, 2020, 56(291), 138-149

ABSTRACT

The velocity distribution of electrons along the symmetry axis is measured by measuring the farther end cap electrode current with negative bias voltage applied across thoriated tungsten filament and alternately through the acquisition of resonance absorption signal of trapped electrons with the storage voltage i.e., for axial motion in a quadrupole Penning trap are presented. Electrons emitted from a thoriated tungsten filament with a range of energies from 1.5eV to 6.5eV are trapped at pressure of 2×10^{-8} torr and magnetic field of 0.05T. In a quadrupole Penning trap thoriated tungsten filament is cathode, closer end cap acts as a grid and farther end cap is the anode. The farther end cap is biased with positive potential respect to the thoriated tungsten filament, the grid is held at zero potential. The first order derivative of the anode current with respect to the grid voltage is directly proportional to Electron energy distribution function of electrons. Alternately, the area under resonance absorption signal of trapped electrons with the storage voltage is plotted. The derivative of area under resonance absorption signal of trapped electrons with the storage voltage is also plotted. Then the derivative of area under resonance absorption signal of trapped electrons with the storage voltage being converted to energy from $E = eV$ is plotted. Now the energy distribution function is transformed to velocity distribution function by converting energy into velocity using the relation $v = \sqrt{2E/m}$. Thus obtained plot is fitted to Gaussian distribution function which is one-dimensional version of Maxwell's velocity distribution function and it is fitted very well. The Gaussian

distribution of velocity is obtained, with a maximum that coincides with the storage potential applied across the thoriated tungsten filament, which is same as that of the velocity distribution of the thermionically emitted electrons from the filament.

Key words: velocity distribution function, quadrupole Penning trap, Maxwell's velocity distribution function, Gaussian distribution function

1. INTRODUCTION

Electrons are confined in Penning trap by the superposition of electric field and magnetic field. The electric field confines electrons in the axial direction through an electric potential minimum and the magnetic field applied along the symmetry axis of the trap confines the electrons in the radial direction. Therefore the trapped electrons have motion in axial direction due to electric field and radial motion due to magnetic field. The Maxwell-Boltzmann distribution law is applicable to identical, indistinguishable particles with any spin (Eg. molecules of gas, trapped electrons under local thermodynamic equilibrium) and the Fermi-Dirac distribution law is applicable to identical, indistinguishable particles with odd-half integral spin that obey Pauli's exclusion principle (Eg. free electrons in a metal). If we assume the electrons inside the trap penetrating into thermal ensembles, then we find Maxwellian velocity distribution for electron-electron collision time $\approx 10\mu s$ under local thermodynamic equilibrium [1,2,3].

When the bias voltage applied across the thoriated tungsten filament is increased at a constant filament current, the energy of the electrons entering the Quadrupole Penning trap increases, then the flux of low-energy electrons that are trapped is reduced and trapping signal disappears gradually. However, if we increase the filament current at the constant bias voltage, the flux of low-energy electrons increases and the trapping signal gradually restored. The resonance absorption signals of detected electrons appear, as electrons reach farther end cap electrode of the trap and those electrons whose energies lower than the trap potential are confined. When the bias is increased gradually at the constant filament current there is a loss of signal and disappears. The signal is restored when filament current is increased at the constant bias voltage. The increase in number density with the increase in flux of trapped electrons causes the space charge induced effects and the signal vanishes completely, that indicates no trapping [4]. Even though the expected distribution function of thermionic electrons is Fermi-Dirac distribution [5], the distribution function obtained from the current measured on the farther end cap electrode results from the electrons that have travelled through the trapping region. The distribution function is expected to change due to the effects of imperfections in quadrupole geometry and collisions of electrons with the background gases in the trap. However, in these situations, thermalization processes, yielding a Maxwell distribution for electron-electron collision time $\approx 10\mu s$, occur on a much shorter time scale [1] than it takes for the electrons to reach the farther end cap, for typical number densities of $10^{15}\ m^{-3}$ and energies of a few eV in the trap [6].

A graph of area under the detection signal is plotted versus the storage voltage. The area under the resonance absorption signal of electrons is directly proportional to the number of electrons trapped in ion trap. The derivative of area under the resonance absorption signal of electrons versus the storage voltage gives the energy distribution function. The data obtained is fitted to a Gaussian function and it is found to fit very well [3,6,7]. The energy is transformed to the velocity using the relation $v = \sqrt{2E/m}$. The graph of derivative of area under the resonance absorption signal of electrons versus velocity yields the velocity distribution of trapped electrons along the symmetry axis of the trap under axial oscillations. The velocity distribution is the Maxwell-Boltzmann distribution along the symmetry axis of the trap and in one-dimension which is a Gaussian distribution function.

The velocity distribution function of trapped electrons obtained through the measurement of the energy of the axial oscillations in a quadrupole Penning trap. Electrons of energies ranging from 1.5eV to 6.5eV are emitted from a thoriated tungsten filament and are trapped at the pressure 2×10^{-8} torr under magnetic field of 0.05T. Subsequently the trapped electrons are detected through monitoring their axial oscillations by an electronic tank circuit that is weakly coupled to the trap, by resonant energy transfer to the electrons. The Lab VIEW program technique developed enables us the direct measurement of the velocity distribution function of the electrons along the symmetry axis of the trap under axial oscillations. We obtain a normal distribution of velocity, with a maximum that coincides with the potential applied across the thoriated tungsten filament that thermionically emits electrons, indicates that the velocity distribution of electrons in the trap reflects the velocity distribution of the thermionically emitted electrons from the filament [3].

2. THEORY

According to Maxwell, at a given temperature when the identical, indistinguishable particles are in thermal equilibrium, then the random motion can be grouped. The velocity distribution function $f(v)$ gives the probability of velocities of particles that can occupy each state of velocity ranging from v and $v + dv$. When the initial minimum energy $E_i > kT$, the Bose-Einstein and the Fermi-

Dirac distribution laws reduce to Maxwell-Boltzmann distribution law. The Maxwell's velocity distribution is skewed as it is not symmetric in velocity and given by [8].

$$f(v) = \frac{dn_v}{n} = \left(\frac{m}{2\pi k_B T}\right)^{\frac{3}{2}} 4\pi v^2 \exp\left[-\left(\frac{mv^2}{2k_B T}\right)\right] \quad (1)$$

For an electron the velocities at a temperature of $10000K$ are

$$v_{mp} = \sqrt{\frac{2k_B T}{m}} = 5.5 \times 10^5 ms^{-1}, \bar{v} = \sqrt{\frac{8k_B T}{\pi m}} = 6.2 \times 10^5 ms^{-1}, v_{rms} = \sqrt{\frac{3k_B T}{m}} = 6.7 \times 10^5 ms^{-1} \quad (2)$$

$$v_{mp} : \bar{v} : v_{rms} = 1 : 1.13 : 1.22$$

The velocity $\boldsymbol{v}$ has components $\boldsymbol{v_x}, \boldsymbol{v_y}$ *and* $\boldsymbol{v_z}$ and the volume element is $d\boldsymbol{v} = d\boldsymbol{v_x} d\boldsymbol{v_y} d\boldsymbol{v_z}$. The kinetic energy of particles in all the three-directions is

$$\frac{1}{2}mv^2 = \frac{1}{2}mv_x^2 + \frac{1}{2}mv_y^2 + \frac{1}{2}mv_z^2 \quad (3)$$

When we introduce the functions $\phi(v_x), \phi(v_y)$ and $\phi(v_z)$ such that

$$\phi(\boldsymbol{v_x}) = \left(\frac{m}{2\pi k_B T}\right)^{\frac{1}{2}} exp\left(-\frac{m{v_x}^2}{2k_B T}\right), \phi(\boldsymbol{v_y}) = \left(\frac{m}{2\pi k_B T}\right)^{\frac{1}{2}} exp\left(-\frac{m{v_y}^2}{2k_B T}\right) \;\&\; \phi(\boldsymbol{v_z}) = \left(\frac{m}{2\pi k_B T}\right)^{\frac{1}{2}} exp\left(-\frac{m{v_z}^2}{2k_B T}\right) \quad (4)$$

$$f(v) = \frac{dn_v}{n} = \phi(v_x)\phi(v_y)\phi(v_z) = \left(\frac{m}{2\pi k_B T}\right)^{\frac{3}{2}} 4\pi v^2 \exp\left[-\left(\frac{mv^2}{2k_B T}\right)\right] \quad (5)$$

The above particle velocity distributions are called Maxwell distributions. The average kinetic energy of particles along different directions is

$$\frac{1}{2}m\langle v^2\rangle = \frac{1}{2}m\langle v_x^2\rangle + \frac{1}{2}m\langle v_y^2\rangle + \frac{1}{2}m\langle v_z^2\rangle = \frac{3}{2}m\langle v_x^2\rangle = \frac{3}{2}m\langle v_y^2\rangle = \frac{3}{2}m\langle v_z^2\rangle \quad (6)$$

Now, the average kinetic energy along x, y and z are equal according to the principal of equipartion of energy.

$$\therefore \frac{1}{3}\left[\frac{1}{2}m\langle v^2\rangle\right] = \frac{1}{2}m\langle v_x^2\rangle = \frac{1}{2}m\langle v_y^2\rangle = \frac{1}{2}m\langle v_z^2\rangle = \frac{T}{2} \quad (7)$$

$$\frac{1}{2}m\langle v_z^2\rangle = \frac{\int_{-\infty}^{+\infty} \frac{1}{2}mv_z^2 exp\left[-\frac{1}{2}\frac{mv_z^2}{k_B T}\right] dv_z}{\int_{-\infty}^{+\infty} exp\left[-\frac{1}{2}\frac{mv_z^2}{k_B T}\right] dv_z} = \frac{T}{2} \quad (8)$$

Thus, the particle kinetic energy per degree of freedom is $^T/_2$, and correspondingly the average kinetic energy of particle in the three-dimensional space is $^1/_2\, m\langle v^2\rangle = {}^{3T}/_2$. These relations define the temperature and hence average kinetic energy of particles [9]. The velocity distribution of electrons along the symmetry axis of the trap, which are under axial oscillations and velocity range between v_z and $v_z + dv_z$ is a Gaussian distribution function given by [9]

$$f(v_z) = \sqrt{\frac{m}{2\pi k_B T}}\left[exp\left(-\frac{m{v_z}^2}{2k_B T}\right)\right] \quad (9)$$

The probability of finding an electron whose energy range between E_z and $E_z + dE_z$ along the symmetry axis of the trap is

$$d\mathcal{P}_z(E_z) = \frac{1}{k_B T} exp\left[-\left(\frac{E_z}{k_B T}\right)\right] dE_z \quad (10)$$

The probability density of an electron whose energy range between E_z and $E_z + dE_z$ along the symmetry axis of the trap is [10]

$$\rho_z(E_z) = \frac{1}{k_B T} exp\left(-\frac{E_z}{k_B T}\right) \quad (11)$$

The average energy of an electron along the symmetry axis of the trap is

$$\langle E_z \rangle = \int_0^\infty E_z \rho_z(E_z) dE_z = k_B T \approx 1.38 \times 10^{-19} J \quad (12)$$

The form of three dimensional quadrupole electric potential is [11,12]

$$V(x,y,z) = \frac{V_0}{r_0^2 + 2z_0^2}(2z^2 - x^2 - y^2) \quad (13)$$

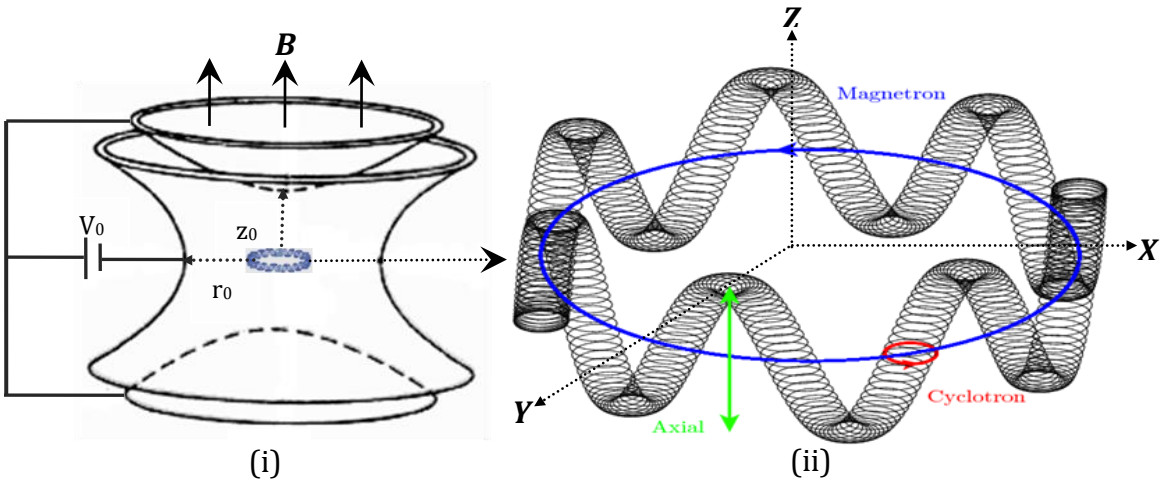

Fig. 1(i)**:** Penning trap, $\boldsymbol{B}$: Magnetic Field, V_0: storage voltage, (ii) Magnified view of motion of an electron in a Penning trap showing reduced cyclotron, magnetron and axial motions

The vector potential of the magnetic field $\boldsymbol{B}$ is [9]

$$\boldsymbol{A} = \frac{1}{2}(\boldsymbol{B} \times \boldsymbol{r}) = \frac{1}{2}B(-y\hat{\boldsymbol{x}} + x\hat{\boldsymbol{y}}), \boldsymbol{E} \times \boldsymbol{B} = \frac{4V_0}{d^2}\dot{x}\hat{\boldsymbol{x}} + \frac{4V_0 B}{d^2}\dot{y}\hat{\boldsymbol{y}} - \frac{2V_0}{d^2}(x\dot{x} + y\dot{y})\hat{\boldsymbol{z}} \quad (14)$$

The Lorenz force in an electromagnetic field with an electric field $\boldsymbol{E}$ and magnetic field $\boldsymbol{B}$ on electron of mass m, charge e, moving with a velocity $\boldsymbol{v}$, is given by [9]

$$\boldsymbol{F} = e[\boldsymbol{E} + (\boldsymbol{v} \times \boldsymbol{B})] \quad (15)$$

$$\boldsymbol{F} = e\left[\left(\frac{2V_0}{d^2}x\hat{\boldsymbol{x}} + \frac{2V_0}{d^2}y\hat{\boldsymbol{y}} - \frac{4V_0}{d^2}z\hat{\boldsymbol{z}}\right) + B(\dot{y}\hat{\boldsymbol{x}} - \dot{x}\hat{\boldsymbol{y}})\right] \quad (16)$$

The potential well due to the electric field in the axial direction causes harmonic oscillations of an electron with frequency given by [11,12]

$$f_z = \frac{1}{2\pi}\sqrt{\frac{4eV_0}{md^2}} \quad (17)$$

An electron in magnetic field performs a cyclotron oscillations in the absence of electric quadrupole field with cyclotron frequency given by [9,11,12]

$$f_c = \frac{eB}{2\pi m} \quad (18)$$

The defocusing electric force modifies the oscillations of electron. The net force experienced by an electron in an electromagnetic field is balanced by the centrifugal force [9,11,12].

$$\therefore \frac{mv^2}{r} = evB - \frac{2eV_0}{d^2}r \tag{19}$$

$$\omega^2 - \omega_c\omega + \frac{\omega_z^2}{2} = 0 \tag{20}$$

$$f_{\pm} = \frac{f_c \pm \sqrt{f_c^2 - 2f_z^2}}{2} \tag{21}$$

The reduced cyclotron frequency is [9,11,12]

$$f_c^{'} = \frac{f_c + \sqrt{f_c^2 - 2f_z^2}}{2} \tag{22}$$

This arises due to the oscillations of the electron in presence of bulk of electrons. The magnetron frequency is [9,11,12]

$$f_m = \frac{f_c - \sqrt{f_c^2 - 2f_z^2}}{2} \tag{23}$$

This corresponds to $(\boldsymbol{E} \times \boldsymbol{B})$ drift in the radial plane around the central region of the trap.

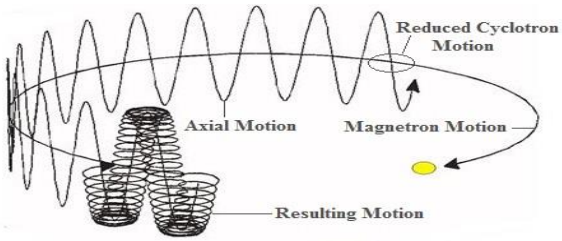

Fig.2: Resulting motion of an electron due to the combination of reduced cyclotron, magnetron and axial motions

V_0 (V)	B (T)	f_c (MHz)	$f_c^{'}$ (MHz)	f_m (MHz)	f_z (MHz)
$4V$	$0.05T$	1399.164	1398.90675	0.5145	26.8288

Table 1: Values of frequencies of an electron due to reduced cyclotron, magnetron and axial motions

$$f_m : f_z : f_c^{'} \approx 1 : 52 : 2719$$

3. EXPERIMENTAL PROCEDURE

Measurement of velocity distribution of trapped electrons along the symmetry axis of the trap: The resistively heated thoriated tungsten filament emits electrons due to thermionic emission and all emitted electrons enter the trap volume through a small orifice of size 3mm in closer end cap, they can travel and reach the farther end-cap electrode of the trap [3,7]. The current on the farther end-cap is due to the electrons emitted by the filament irrespective of their kinetic energy. The integration of the electron energy distribution function $f(E_z)$ of thermionic electrons at farther end-cap represents all energy values. At lower bias voltages the electrons of low kinetic energy do not reach the end cap. The bias voltage is reduced till zero value; the current is obtained due to electrons with kinetic energy of an upper bound of the energy due to the bias voltage. The filament bias is varied between 1.5V to 6.5V that causes the entry of electron into the trap having different velocity distributions centered around the bias voltage are trapped. The energy of electrons is a few eV and the temperature of electrons is around 10000K which is much greater than the surrounding neutral gas molecules whose temperature is around 300K. The electron plasma generated is non-thermal plasma under local thermodynamic equilibrium. In this experiment electron-electron collision time $\tau_{ee} \approx 10\mu s$ during which local thermal equilibrium is achieved [3], which is much smaller than the time (few tens of milliseconds) during which the measurements are carried out and hence we are probing the regime wherein the electron plasma has reached local thermodynamic equilibrium [3,9]. We find Maxwellian velocity distribution, for electron-electron collision time $\approx 10\mu s$, when the electrons inside the trap

penetrating into thermal ensembles [1,3,9]. The graph of farther end cap electrode current versus negative bias voltage applied across the filament, and alternately the graph of area under detection signal of electrons versus storage potential is similar to the I-V curves obtained using Langmuir probes and yield energy distribution function and hence velocity distribution function.

(i) Measurement of velocity distribution from farther end cap electrode current: In a quadrupole Penning trap thoriated tungsten filament is cathode, closer end cap acts as a grid and farther end cap is the anode. The farther end cap is biased with positive potential respect to the thoriated tungsten filament, the grid is held at zero potential. The farther end cap electrode current is measured with the variation of negative bias voltage from 1.5V to 6.5V which is applied across the thoriated tungsten filament to trap electrons. The first order derivative of the anode current with respect to the grid voltage is directly proportional to Electron energy distribution function of electrons [13,14]. The anode current I decreases with decrease in bias voltage from V to $V-\Delta V$, then electrons whose energies $E < eV$ do not reach the farther end cap electrode. Energy distribution function of electrons is obtained from the first order derivative of the anode current with respect to the grid voltage [3,15]. The reduction in current at the farther end cap is [15]

$$\delta N = \delta I = e\int_{V}^{\infty} f(E_z)\,dE_z - e\int_{(V-\Delta V)}^{\infty} f(E_z)\,dE_z \tag{24}$$

$$\left|-\frac{1}{e}\right|\frac{dI}{dV} = \frac{1}{e}\frac{dI}{dV} = f(E_z) \qquad \left\{\because N = \left|\frac{I}{e}\right| = e\int_{0}^{\infty} f(E_z)\,dE_z\right\} \tag{25}$$

(ii) Measurement of velocity distribution from Resonance absorption signal strength: The detection of electrons is achieved by coupling the trap to a weakly excited detection circuit using a non-destructive detection technique. The confinement times of electrons in the quadrupole Penning trap in our experiments are in the range of few tens of milliseconds as shown in Fig.3, which is much greater than the time for the entry of the electrons into the trap to achieve the local thermal equilibrium which is around $10\mu s$.

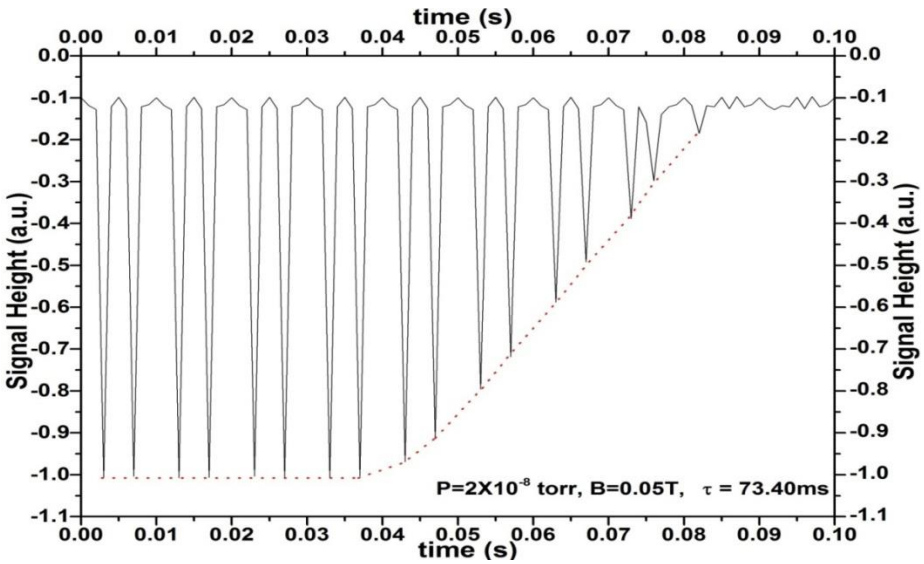

Fig.3: Signal fall-off with time with confinement time, $\tau = 73.40\ ms$, at pressure $P = 2\times10^{-8}$ torr, and magnetic field $B = 0.05\ T$

The potential V is reduced to $V' = V - \Delta V$, and then the electrons with energies $E_z < eV$ trapped only, then ΔN be the number of reduction in trapped electrons. The number of electrons trapped at the trap voltage $V$is [3,9,15]

$$\Delta N = e\int_{0}^{eV} f(E_z)\,dE_z - e\int_{0}^{e(V-\Delta V)} f(E_z)\,dE_z \tag{26}$$

Taylor expansion around eV, considering only first order term, neglecting higher order terms

and taking limit as $\Delta V \rightarrow 0$ yields

$$\lim_{\Delta V \to 0} \frac{\Delta N}{\Delta V} = \frac{dN}{dV} = f(E_z) \tag{27}$$

The derivative of the area under the resonance absorption signal of trapped electrons versus energy of electrons is plotted and slope of the curve gives the Maxwell-Boltzmann distribution function [3,9]. The graph yields the energy distribution and hence velocity distribution of trapped electrons along the symmetry axis of the trap as we measure only the axial motion [3,9]. The graph of the data is fitted to the following form of Gaussian distribution which is one-dimensional version of Maxwell-Boltzmann distribution for electrons trapped in ion trap [9].

$$y = y_0 + \frac{A}{w\sqrt{\pi/2}} exp\left[-2\left(\frac{x - x_c}{w}\right)^2\right] \tag{28}$$

Electrons are loaded into the trap whose energy is distributed around the filament bias voltage, which is varied from 1.5 to 6.5 V that determines the energy and hence velocity of the electrons. Initially the storage potential is held at 6.5 V and then reduced to a potential V as shown in Fig. 4, which causes electrons with energy higher than V leaving the trap. After a certain time t, the detection of trapped electrons is carried out and the resulting signal strength is recorded. The measurements are made continuously by reducing the potential V in steps of 0.5 V, this voltage may be reduced to a minimum of 1.5 V. The loading of electrons into the trap volume is terminated by gradually reducing the filament bias to 1V. No detection is observed below this voltage as the storage potential cannot be lower than the detection potential, when no electrons are trapped. Then the electrons of all energies enter the trap, but those electrons whose energy is lower than the trap voltage are trapped. The potential is reduced to V, then the electrons whose energies greater than eV leave the trap. The time called the dwell time, during which the trap voltage remains V, then the electrons whose energies exceed eV escape from the trap. The dwell time is well within the confinement time of the trapped electrons. The voltage is then ramp down, and then the axial frequency of the trapped electrons is varied. At a certain ramp voltage the corresponding axial frequency matches the tuned detection circuit frequency, then the energy is transferred from the detection circuit to the electrons and the corresponding signal of electrons obtained is recorded.

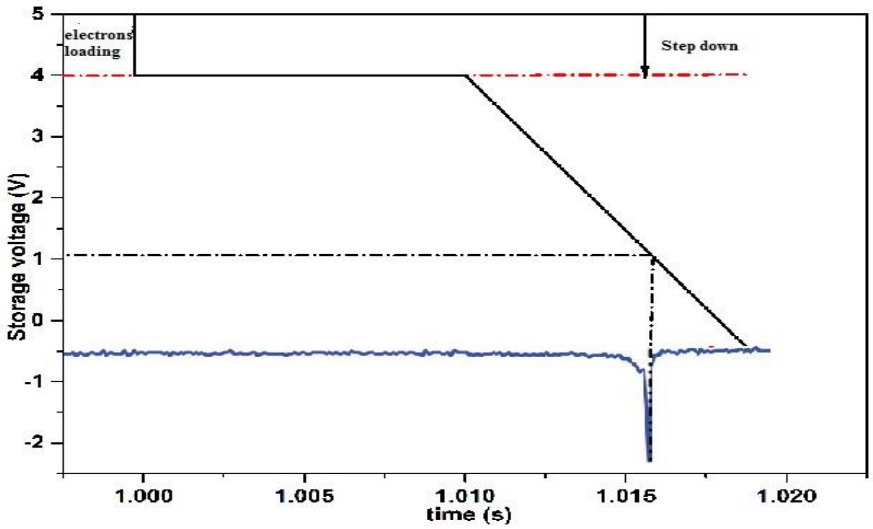

Fig.4: Schematic diagram showing the variation in applied storage voltage with time. The electrons are injected in to the trap for 1s, and signal of electrons appears when the trap potential is ramped.

When the detection circuit was tuned to an axial oscillation frequency that corresponded to about 1V, the resonant energy transfer takes place from the circuit to the trapped electrons; therefore the minimum storage voltage is set at 1.5V. Measurements on energy and hence velocity along symmetry axis of the trap are carried out for different storage voltages; the strength of resonance absorption signal of electrons is directly proportional to the number of electrons trapped and are recorded.

4. RESULTS AND ANALYSIS

(i) Measurement of velocity distribution from farther end cap electrode current: The thermally generated electrons are accelerated, and then pass through the center of the trap and reach farther end cap electrode which results current. The negative bias voltage was varied from 1.5V to a maximum of about 6.5V in steps of 0.5V and the farther end cap electrode current was recorded at each bias voltage. All the electrons emitted by the process of thermionic emission from the thoriated tungsten filament can travel and reach the farther end cap electrode; the current is due to all the electrons being emitted irrespective of their kinetic energy. The farther end cap current is due to the energy distribution function $f(E_z)$ of the thermionic electrons over all energy values range between E_z and $E_z + dE_z$ along the symmetry axis of the trap. At lower bias voltages the electrons which have low kinetic energy do not reach the farther end cap. The electrons at 0V bias voltage, the kinetic energies have an upper bound of the energy due to the bias voltage. A graph of farther end cap electrode current versus the negative bias voltage applied across the thoriated tungsten filament is plotted, which shows that if there is no bias voltage on the farther end cap electrode there is zero current, when the bias is increased then the current increases gradually and reaches almost a constant value. A graph of farther end cap electrode current versus the negative bias voltage is plotted as shown in Fig. 5.

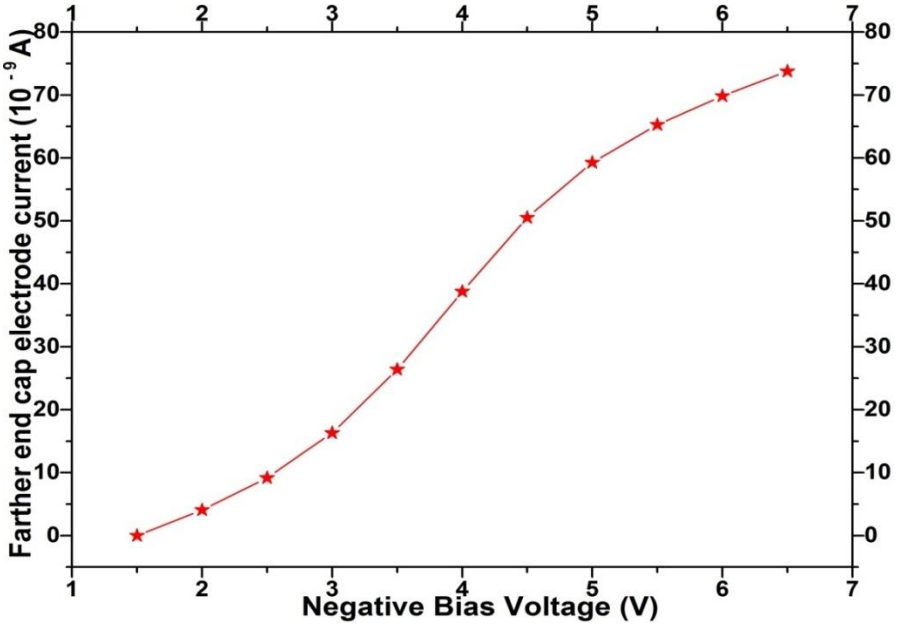

Fig.5: Farther end cap electrode current versus negative bias voltage for electrons

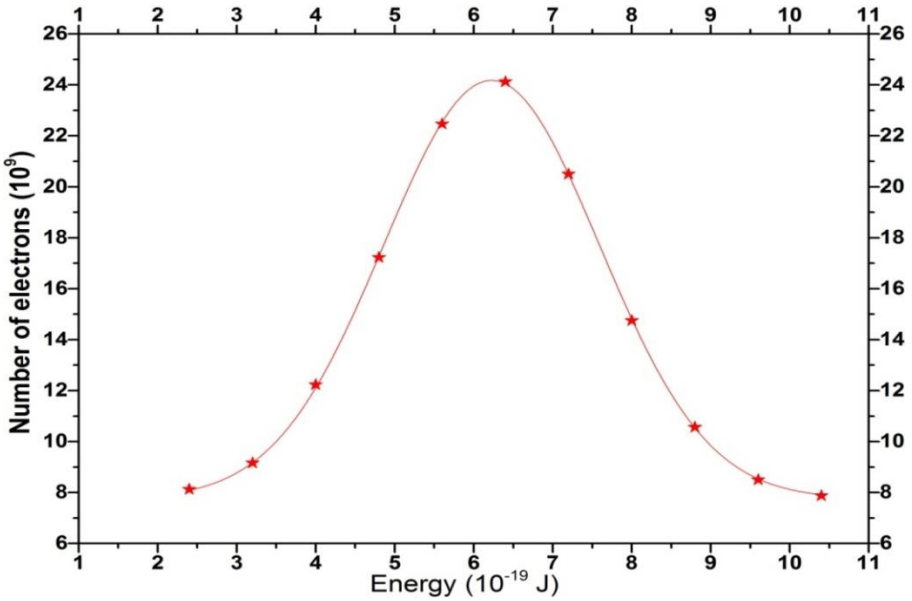

Fig.6: Energy distribution of electrons measured from farther end cap electrode current

The farther end cap electrode current is converted into number of electrons using $N = I/e$ and the negative bias voltage is converted into energy of electrons using $E = eV$. A graph of number of electrons versus energy of electrons is plotted, which shows the energy distribution of thermal electrons as shown in Fig. 6. The energy of electrons is converted into velocity using $v = \sqrt{2E/m}$ and a graph of number of electrons versus velocity of electrons is plotted, which shows the velocity distribution of thermal electrons as shown in Fig. 7.

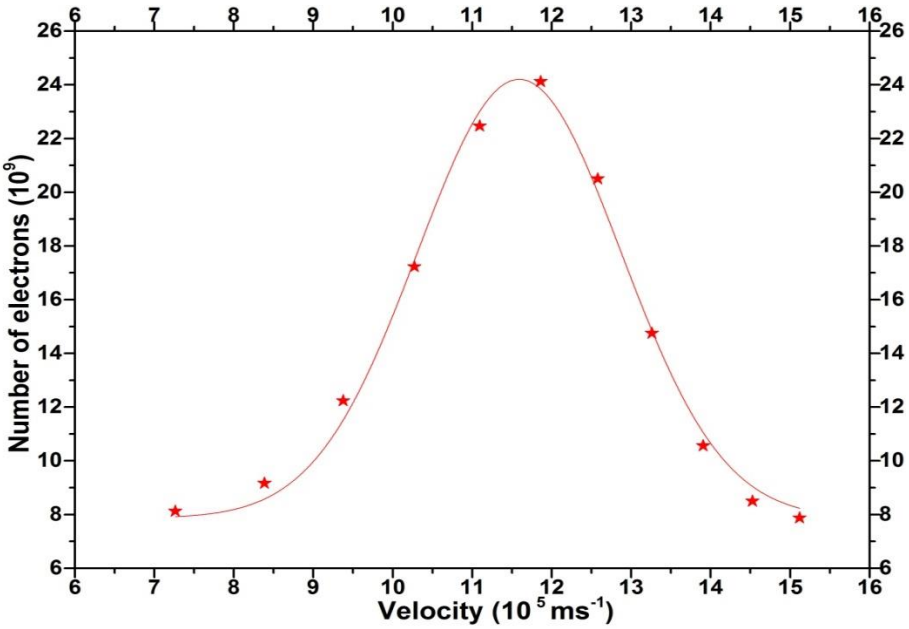

Fig.7: Velocity distribution of electrons measured from farther end cap electrode current

(ii) Measurement of velocity distribution from Resonance absorption signal strength: The detection signal of electrons appears as soon as electrons enter the trap; the electrons which have energies lower than the trap potential are confined. When the bias is gradually increased, at the constant filament current, there is a loss of signal. At constant bias the signal is restored when the filament current is gradually increased. The restored signal is now at a different trap voltage on the ramp, when it is compared to the previous measurement. The trapping voltage shifts significantly with the variation of bias, due to the variation of the number of trapped electrons, this indicates the effect of space charge in shifting the trapping potential [16]. The appearances and disappearances of the signal alternately, when the bias voltage is varied is due to the velocity distribution of the electrons which are entering the trap. Thermalization processes that yield a Maxwell distribution due to electron-electron collisions, for typical number densities of $10^{15}\ m^{-3}$ and energies of a few eV in the trap which occurs on a much longer time scale than it takes for the electrons to reach the farther end cap. The axial oscillation frequency of the electrons is modified by space charge effects of cloud of electrons. The signal of trapped electrons is acquired and the area under the signal is found for different storage voltages. The area under the resonance absorption signal of trapped electrons is directly proportional to the total number of trapped electrons [3,9]. The number of electrons at the centre of the trap is measured using non-destructive detection technique at different trapping potentials. The axial oscillatory motion of the electrons is controlled through the Lab VIEW program that controls storage voltage. The number of electrons at the centre of the trap depends upon the storage potential. A graph of area under the detection signal is plotted against the storage voltage as shown in Fig. 8. The graph shows that the area under detection signal increases gradually and has plateau region beyond 6V.

The derivative of the area under the resonance absorption signal of trapped electrons is plotted against the storage voltage and the function is fitted to a Gaussian function as shown in Fig.9 [3,9,17]. The storage voltage is converted into energy of electrons using $E = eV$ and the graph of the derivative of the area under the resonance absorption signal of trapped electrons is plotted against the energy of electrons and the function is fitted to a Gaussian function which shows the energy distribution function $f(E_z)$ measured along the symmetry axis of the trap at the pressure of 2×10^{-8} torr and the magnetic field of 0.05T and as shown in Fig.10.

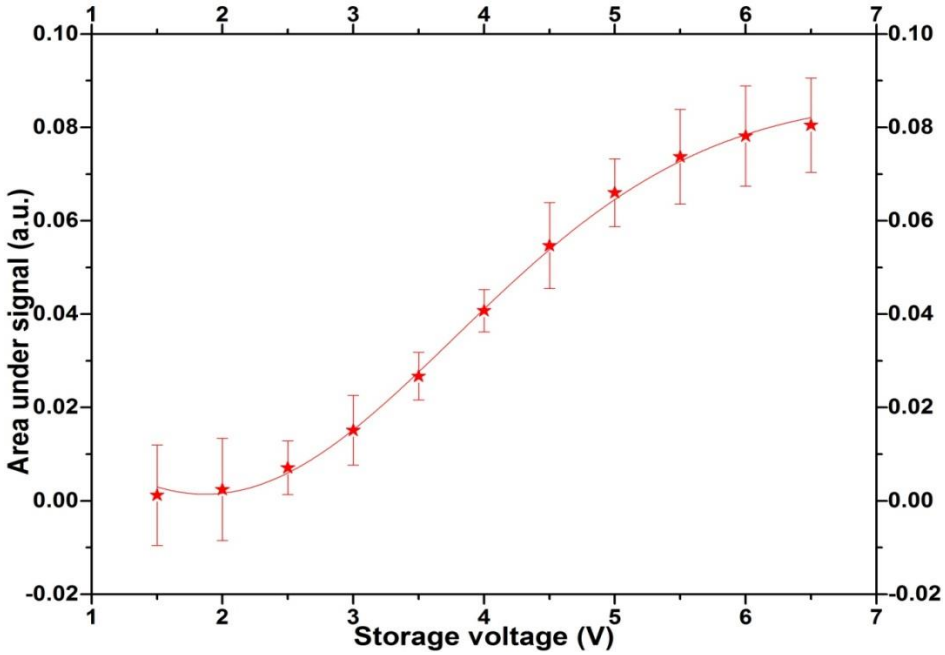

Fig.8: Variation of area under signal with storage voltage at the pressure of 2×10^{-8} torr and magnetic field of 0.05T

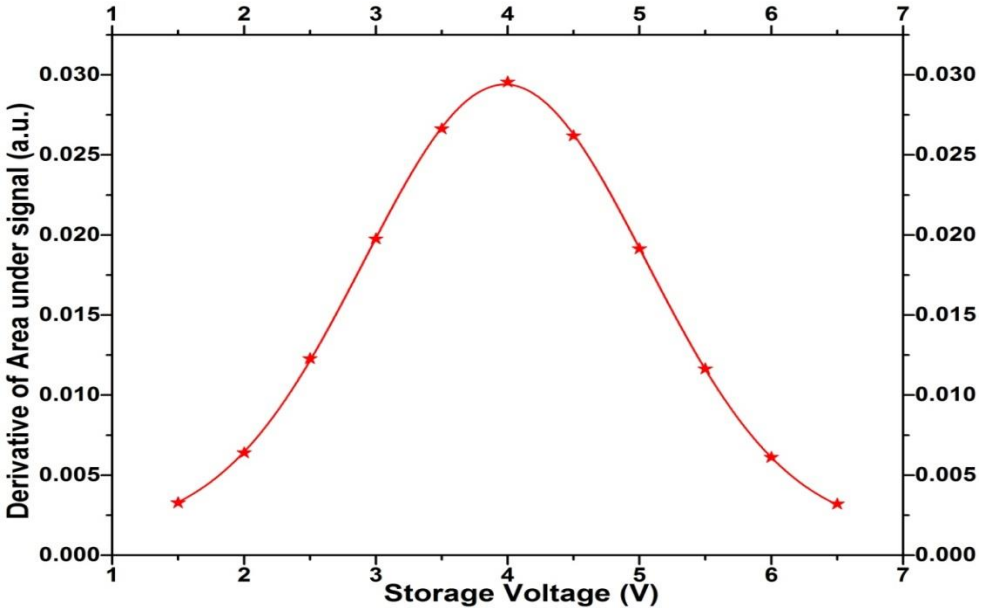

Fig.9: Variation of derivative of the area under the detection signals versus storage voltage at the pressure 2×10^{-8} torr and magnetic field of 0.05T

The energy of electrons is converted into velocity using $v = \sqrt{2E/m}$ and a graph of derivative of the area under the resonance absorption signal of trapped electrons versus velocity of electrons is plotted, which shows the velocity distribution of thermal electrons $f(v_z)$ measured along the symmetry axis of the trap at the pressure of 2×10^{-8} torr and the magnetic field of 0.05T and as shown in Fig.11 [3,9].

Fig. 5 is the graph of area under the detection signal versus storage voltage and Fig. 6 is the corresponding derivative of the area under the detection signal versus storage voltage, which shows the energy distribution function.

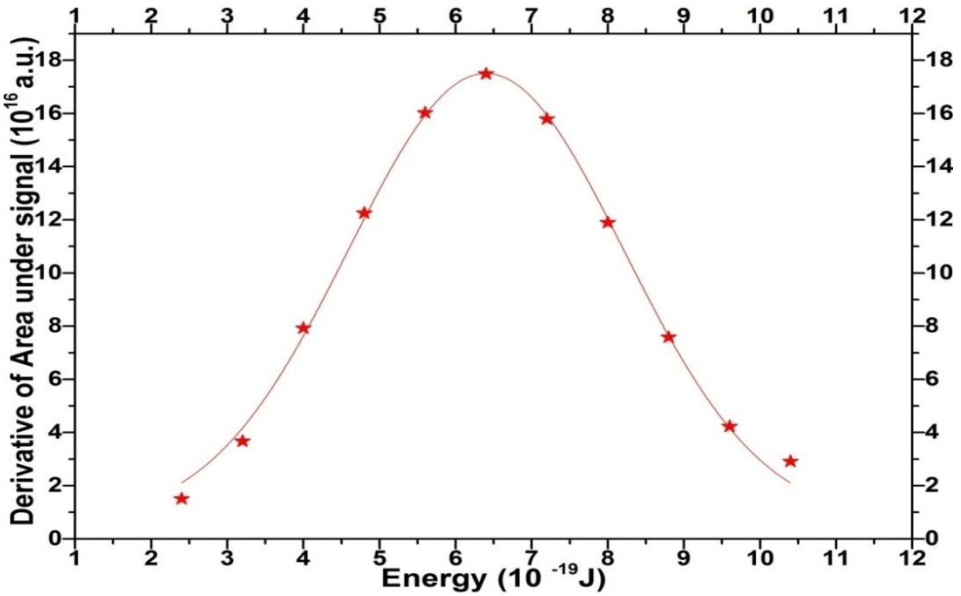

Fig.10: Variation of derivative of the area under the detection signals versus energy at the pressure 2×10^{-8} torr and magnetic field of 0.05T

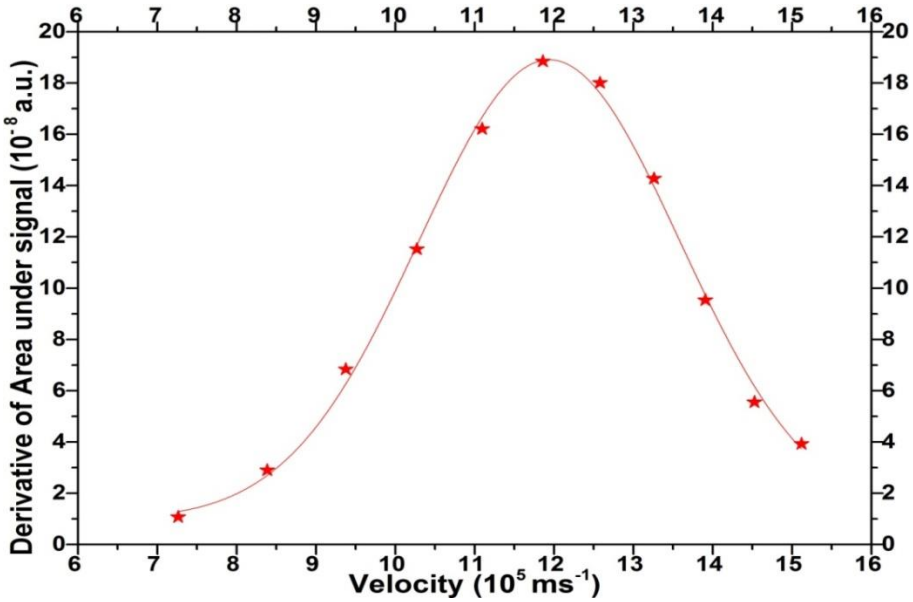

Fig.11: Variation of derivative of the area under the detection signals versus velocity at the pressure 2×10^{-8} torr and magnetic field of 0.05T

5. CONCLUSION

The trapped electrons that form non neutral, non thermal plasma are in local thermodynamic equilibrium under low pressure of $\sim 2 \times 10^{-8}$ torr and magnetic field of 0.05T. The strength of the detection signal of electrons varies with the storage voltage and this variation depends on the range of velocities of electrons due to the bias voltages applied across the filament. However, the variation of detection signal of electrons along the symmetry axis of the Quadrupole Penning trap is independent of the applied external magnetic field. This demonstrates the possibility of the direct measurement of the distribution function of the velocity along the symmetry axis of the trap and it is monitored through detection of resonance absorption signal in non-destructive electronic detection technique. The axial oscillatory motion of trapped electrons along the symmetry axis of the Quadrupole Penning trap is decoupled from their radial motion, under local thermodynamic equilibrium condition; therefore the velocity distribution function of the trapped electrons can be measured along the symmetry axis of the trap. It was found that the most probable energy of electrons is 4eV which is approximately 50% of the potential depth of the trap. The velocity distribution function shows that the maximum is

at the storage voltage that corresponds to the bias voltage across the thoriated tungsten filament. Thus, the distribution function of the electrons reflects the total velocity distribution measured along the symmetry axis of the trap, independent of the fact that whether we monitor only the axial motion, due to the consequence of equipartition of energy in all degrees of freedom of motion.

REFERENCE

1. A.Dinklage, T. Klinger, G. Marx, L. Schweikhard, *Plasma Physics*, (Springer 2008)
2. U. Schumacher, '*Basics of Plasma Physics'*, (Springer) P13
3. Durgesh Datar, Dyavappa B M, Mahesh B L, K T Satyajith, Sharath Ananthamurthy. *'Energy distribution of electrons under axial motion in a quadrupole Penning trap'*. Can. J. Phys (2016), 1245-1249
4. Winters D F A, Vogel M, Segal D M, et al. 2006, J. Phys. B, 39: 3131
5. Azooz A A. 2007, Eur. J. Phys., 28: 635
6. Soumen Bhattacharya, Anita Gupta, S G Nakhate and Pushpa M Rao, BARC Mumbai, *'Measurement of storage time, estimation of ion number and study of absorption line profile in a Paul trap'*(2006)
7. K T Satyajith, Anita Gupta, Gopal Joshi, Shyam Mohan, Pushpa Rao and Sharath Ananthamurthy, '*Loading Detection and Number Estimation of an Electron Plasma in a Penning Trap',* Plasma Science and Technology, Vol. 11, No. 5, 2009, P.521-528.
8. Robert C. Dunbar, '*Deriving the Maxwell distribution'*, *Journal of Chemical Education* 1982 *59* (1), 22 DOI: 10.1021/ed059p22
9. Dyavappa B M, '*Spectroscopy of non-neutral plasmas in ion traps'* (Ph.D. thesis, 2017)
10. Guo-Zhong Li, G.Werth, *'Energy distribution of ions in Penning trap'*, Int.J.Mass Spectro. Ion Processes, 121 (1992), 65-75.
11. F.G.Major, V.N.Gheorghe, G.Werth, *'Charged Particle Traps'*, *Physics and techniques of charged particle confinement*, (Springer) -2005
12. Pradip K.Ghosh, *'Ion Traps',* Clarendon Press, Oxford (1995), P72
13. Popov, T.K., Ivanova, P., Dimitrova, M., Stockel, J. & Dejarnac, R.. '*On the first derivative probe method for electron energy distribution function measurements in tokamak edge plasma'*. Journal of Physics: Conference Series, (2008), 113, 012004. 53
14. Shariatzadeh, R., Emami, M., Ghoranneviss, M. & Fard, A.A.T. (2010). Recent results of edge plasma parameters measurements in IR-T1 tokamak by probe. Journal of Fusion Energy, 29, 271-274. 53
15. K.T.Sathyajith, PhD thesis (2010), *'Spectroscopy of electrons and ions in electromagnetic traps'*
16. Jeffries, J., Barlow, S. & Dunn, G. (1983). '*Theory of space-charge shift of ion cyclotron resonance frequencies'*. International Journal of Mass Spectrometry and Ion Processes, 54, 169, 187, 50
17. Gaussian Distributions © By Kevin Lehmann Princeton University, & Chris Williams, School of Informatics, University of Edinburgh